Spatial Patterns and Age-Related Changes of the Collagen Crimp in the Human Cornea and Sclera

Alexandra Gogola,[1] Ning-Jiun Jan,[1,2] Bryn Brazile,[1] Po Lam,[1] Kira L. Lathrop,[1,2] Kevin C. Chan,[1,3,4] and Ian A. Sigal[1,2]

[1]Department of Ophthalmology, University of Pittsburgh, Pittsburgh, Pennsylvania, United States
[2]Department of Bioengineering, University of Pittsburgh, Pittsburgh, Pennsylvania, United States
[3]Department of Ophthalmology, New York University, New York, New York, United States
[4]Department of Radiology, New York University, New York, New York, United States

Correspondence: Ian A. Sigal, Laboratory of Ocular Biomechanics, Department of Ophthalmology, University of Pittsburgh School of Medicine, 203 Lothrop Street, Room 930, Pittsburgh, PA 15213, USA; ian@OcularBiomechanics.com.

Submitted: November 22, 2017
Accepted: May 2, 2018

Citation: Gogola A, Jan N-J, Brazile B, et al. Spatial patterns and age-related changes of the collagen crimp in the human cornea and sclera. *Invest Ophthalmol Vis Sci*. 2018;59:2987–2998. https://doi.org/10.1167/iovs.17-23474

Purpose. Collagen is the main load-bearing component of the eye, and collagen crimp is a critical determinant of tissue mechanical behavior. We test the hypothesis that collagen crimp morphology varies over the human cornea and sclera and with age.

Methods. We analyzed 42 axial whole-globe sections from 20 normal eyes of 20 human donors, ranging in age from 0.08 (1 month) to 97 years. The sections were imaged using polarized light microscopy to obtain μm-scale fiber bundle/lamellae orientation from two corneal and six scleral regions. Crimp morphology was quantified through waviness, tortuosity, and amplitude.

Results. Whole-globe median waviness, tortuosity, and amplitude were 0.127 radians, 1.002, and 0.273 μm, respectively. These parameters, however, were not uniform over the globe, instead exhibiting distinct, consistent patterns. All crimp parameters decreased significantly with age, with significantly different age-related decreases between regions. The crimp morphology of the limbus changed the most drastically with age, such that it had the largest crimp in neonates, and among the smallest in the elderly.

Conclusions. Age-related decreases in crimp parameters are likely one of the mechanisms underlying age-related stiffening of the sclera and cornea, potentially influencing sensitivity to IOP. Further work is needed to determine the biomechanical implications of the crimp patterns observed. The comparatively large changes in the crimp morphology of the limbus, especially in the early years of life, suggest that crimp in this region may play a role in eye development, although the exact nature of this is unclear.

Keywords: collagen crimp, waviness, tortuosity, amplitude, aging

Collagen fibers are found throughout the globe.[1–3] These fibers exhibit a well-known property of collagen: the fibers are wavy, or crimped.[4–10] As for other collagenous soft tissues,[11–13] crimp in the corneoscleral shell is believed to be a primary determinant of the eye's nonlinear biomechanical behavior, explaining, for instance, that the globe stiffens as IOP increases.[14,15] The biomechanical behavior of the eye, in turn, plays a central role in several potentially blinding conditions and diseases.[7,14,16–18] Age-related stiffening, for example, is thought to contribute to the increased susceptibility to glaucoma in the elderly.[19] Hence, to preserve vision, it is necessary to also understand the collagen fiber crimp over the globe and how it changes with age. However, despite the importance of crimp on eye structure and mechanics, only a handful of studies have specifically looked at collagen crimp in the cornea and sclera in animal eyes,[4,7,9,19–22] and almost nothing is known about collagen fiber crimp in human eyes. This is the gap we address in this work.

The structural and biomechanical demands on the cornea and sclera vary over the globe, and, accordingly, several studies have reported variations in tissue mechanical properties over the globe.[23–26] Hence, it seems reasonable to expect that the microarchitecture of the underlying collagen that determines these properties also varies over the globe. The corneoscleral shell, however, is a continuous, cohesive envelope, in which the regional biomechanics are not independent, but are instead dependent on those of other regions, both nearby and afar.[14,27–29] Hence, it also seems plausible that collagen crimp will exhibit specific patterns over the globe, perhaps even with distant regions having similar properties.

Several studies have reported that the cornea and sclera stiffen with age,[16,18,30] but the processes underlying this stiffening remain unclear. Numerical studies have suggested that the stiffening is in large part due to age-related changes in collagen crimp properties.[18,31] The predictions of the models, however, have not been verified experimentally. In other tissues, age-related changes in collagen fiber crimp, and the consequent tissue stiffening, have been demonstrated.[32–34]

In this work, we report the results of a careful systematic experimental study of the collagen fiber crimp characteristics in the human cornea and sclera. We use these measurements to test the hypothesis that collagen crimp morphology varies over the globe and with age. Specifically, we characterized three aspects of crimp morphology: waviness, tortuosity, and amplitude, and quantify whether these change with age over the globe and regionally. To measure crimp, we used

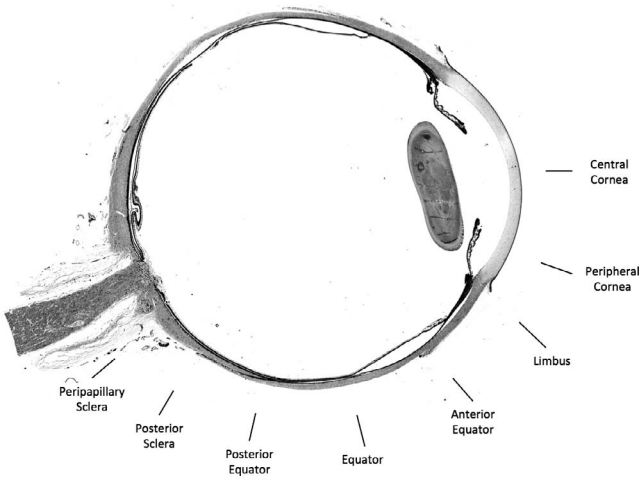

FIGURE 1. Map of eight regions sampled on a whole-globe brightfield image of a section of the eye. We pooled measurements from the 16 corresponding nasal and temporal regions into the eight full regions used for analysis.

techniques based on polarized light microscopy (PLM) that we have recently demonstrated are suitable for direct measurement of crimp in ocular tissues.[21,35]

METHODS

Sample Acquisition and Selection

This study was conducted in accordance with the tenets of the Declaration of Helsinki and the Health Insurance Portability and Accountability Act (HIPAA). Human sections were obtained from the University of Pittsburgh Medical School Department of Pathology. These sections were originally prepared and processed by Pathology for other purposes, with particular attention given to consistent overall tissue handling for all eyes. The sections were de-identified before we received them, meaning all patient information, other than age, sex, and eye condition or pathology, was inaccessible. This was done in compliance with HIPAA and with the institutional review board. Eye condition and pathology were determined by the personnel of Pathology based on clinical records and their own observations from the tissues. Directly after obtaining the eyes, they were fixed in 10% neutral buffered formalin for a week. The globes were bisected into inferior and superior portions, without cutting through the optic nerve head (ONH). The superior portion, containing the ONH, was embedded in paraffin, and 5-μm-thick axial sections through the center of the globe collected. Each section was then prepared with one of six different stains for the purposes of Pathology, although there were no more than four different stains applied to the sections of any one eye. Although we were able to tell the stains apart, the specific stain used on a section was masked by using a code, which we were not given. This required us to do preliminary testing to ensure that the stains did not affect our measurements (more in Supplementary Materials).

Slides were selected for study based on three criteria: the eyes were normal without conditions or pathologies that could alter or compromise connective tissues (e.g., without tumors or high myopia), availability of age information, and good whole-globe section quality. All selected sections were intact whole-globe sections, with no large tears or folds. In the interest of acquiring the most data possible, we used all the sections that satisfied the inclusion criteria, even if this meant different numbers of sections between subjects. The number of sections per subject ranged from one to four. Overall, this resulted in a total of 42 sections from 20 eyes from 20 subjects. The subjects' ages ranged from 0.08 (1 month) to 97 years. There were eight males, eight females, and four of unspecified gender.

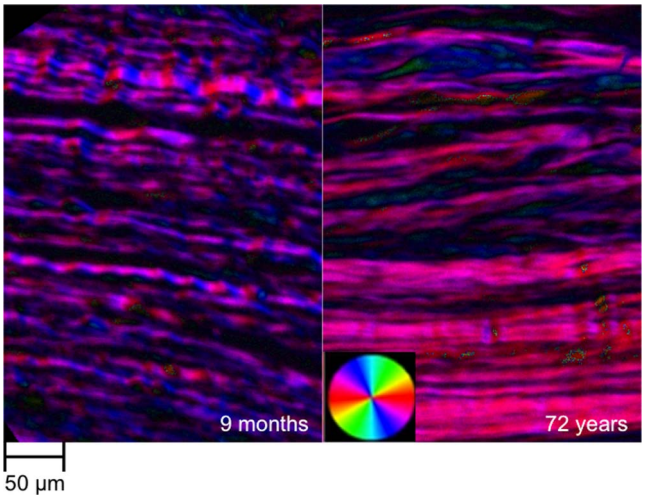

FIGURE 2. Example orientation maps of the limbus from a young (9 months) and an old (72 years) subject. The fiber orientations at each pixel were determined using the four PLM images collected for each sample. The orientation maps were then visualized by color-coding the fiber orientations. The brightness was scaled according to the signal strength at a pixel. The orientation map of the young limbus shows undulations in color along the fibers, showing that the fibers are crimped. The orientation map of the older limbus does not show much variation in orientation, suggesting a reduction of crimp with age.

Image Acquisition

Images were collected from 16 locations around the globe from each section. The corresponding temporal and nasal sides were pooled into eight regions (Fig. 1): central cornea, peripheral cornea, limbus (including the peri-limbus), anterior equator (sclera anterior to the equator), equator, posterior equator (sclera directly posterior to the equator), posterior sclera (sclera of the posterior pole), and peripapillary sclera (PPS). Images from the any of the 16 regions were excluded from analysis if there were small tissue tears or folds apparent in the images.

The selected sections were imaged using PLM with an Olympus BX60 microscope (Olympus, Tokyo, Japan) coupled with a SPOT camera (SPOT Imaging Solutions, Sterling Heights, MI, USA) and a 10× objective (numerical aperture [NA] 0.3) in conjunction with two filters, a polarizer and an analyzer (Hoya, Tokyo, Japan). The resulting images were 12-bit grayscale and had a resolution of 0.73 μm/pixel. Briefly, four images were captured, with filter orientations 45° apart for each successive image. Using a previously reported method,[21,35] and custom code run within Fiji Is Just ImageJ (FIJI) (http://imagej.nih.gov/ij/; provided in the public domain by the National Institutes of Health, Bethesda, MD, USA),[36] the changes in intensity of each pixel were used to calculate the collagen fiber orientation, creating orientation maps (Fig. 2).

Terminology

Collagen hierarchical organization and architecture are complex and vary throughout the eye.[2] In the cornea, there is a lamellar structure made up of highly parallel and evenly spaced fibrils. In the sclera, the fibers form "bundles." A description or

Investigative Ophthalmology & Visual Science

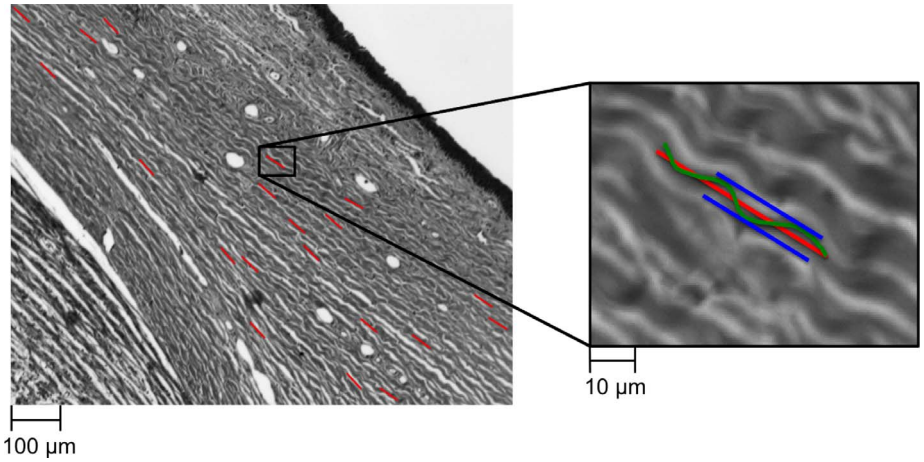

FIGURE 3. Line markings were used to quantify collagen fiber crimp tortuosity, waviness, and amplitude. A few example line markings used for measuring these crimp parameters are shown on the *left panel* (*red lines*) overlaid on a brightfield image. To the *right* is a close up of a marked collagen bundle. Tortuosity was computed as the ratio of fiber path length (*green wavy line*) over the end-to-end length (*red line*); waviness was computed as the circular SD of the fiber orientation along the end-to-end path; amplitude was defined as half the distance from peak to trough within a wave (*blue lines*).

analysis of collagen hierarchy was not the goal of this work. For simplicity, we use the general term "bundle," even though it may have slightly different meaning in the cornea and the sclera.

Crimp Quantification

Crimp parameters were calculated in each region from the collagen fiber orientation in at least 20 fiber bundles, distributed throughout depth, as a preliminary study suggested was necessary to obtain a reliable description of the region. For each collagen bundle, we manually placed a straight-line segment, 60 pixels long (~45 μm) (Fig. 3). These line segments were used to sample the orientation values within the bundles for calculation of the crimp parameters. When marking, we were careful to distribute the marks evenly over a region, and to place them only on well-defined collagen bundles and lamellae that were long and bright. This limits the analysis to fibers in, or close to, the section plane. Elsewhere we have shown that brightness in our PLM images is indicative of the fibers being mostly in the plane of the section.[37]

Three crimp parameters were calculated: waviness, tortuosity, and amplitude. The quantification of these parameters followed the methods described in detail elsewhere.[38] Briefly, waviness was calculated as the circular standard deviation (SD) of the angle values (green line, Fig. 3); tortuosity was calculated as the ratio of the path length to the end-to-end length of a fiber (ratio of green to red, Fig. 3); and amplitude was defined as half the distance between the peak and trough of a wave (half distance between blue lines, Fig. 3). All crimp parameters were calculated using custom code in FIJI.[36]

Calculation of the crimp parameters was based on the fiber orientation values, not from visualization of the physical wave of the fiber (Fig. 4). Waviness, tortuosity, and amplitude were calculated from the array of fiber orientation values, one from each pixel, along the line segment. Waviness was computed as the circular SD of each of the pixels' orientation values. Tortuosity was computed by first computing the path length component of each pixel, then adding these values over the array, to obtain the overall path length. This was then divided by the sum of the end-to-end lengths in each pixel. Amplitude was computed by summing the amplitude component of each pixel. The components were added up to determine amplitude in the positive and negative directions so they could be averaged. The accuracy and robustness of this method were evaluated in a preliminary analysis by comparing the waviness, tortuosity, and amplitude with measurements taken using fiber tracing in simulated fibers, in tendon, and in regions of the eye in which were the crimp is indeed visible. The differences between this method and tracing were within 1.0%, 1.5%, and 2.0% in simulated fibers, tendon, and in limbus, respectively. We also determined that our measure-

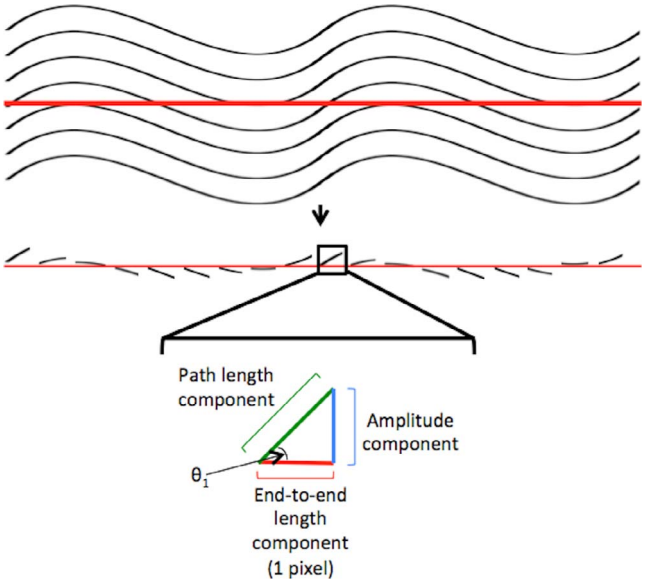

FIGURE 4. Crimp parameter calculation. Computation of the collagen's waviness, tortuosity, and amplitude was based on the fiber orientation value at each pixel along the straight-line segment. Waviness was computed as the circular SD of the pixels' orientation values (θ_1). Tortuosity was computed as the ratio of the sum of the pixels' path length components to the sum of the end-to-end length components. Amplitude was computed as the sum of the pixels' amplitude components, averaging total contributions in positive or negative directions.

ments were robust to changes in the length and angle of the manually marked line. As long as the line was between one and three wave periods, and within 45 degrees of the main collagen bundle direction, the resulting crimp parameters were within 3% of each other.

Statistical Analyses

Sample Number Comparison. ANOVA tests were conducted on five regions from two different subjects to test for differences in waviness, tortuosity, and amplitude associated with the number of collagen bundles sampled (20, 30, 40, and 50) to determine the number of collagen bundles needed to obtain a reliable description of crimp parameters within a region. The parameters were not considered significantly different if they yielded P values greater than 0.1.

Stain Comparison. To assess differences in waviness, tortuosity, and amplitude between measurements obtained from sections with different stains, ANOVA tests were conducted on two previously stained eyes, one with three different stains and another with four different stains. Between the two eyes, all stains were tested, with one stain common to the two to aid in comparison. The measurements therefore incorporate both differences due to stain and inter-section variability. Pairs were not considered significantly different if they yielded P values greater than 0.1.

Global Crimp Parameter Associations With Age. Pooling all of the regions together for each eye, we determined if each of the three crimp parameters decreased or increased monotonically with age. We also assessed if there were significant changes with age. We assessed monotonic changes in the crimp parameters with age using Spearman tests and modeled the age-related changes using linear mixed effects (LME) models, which account for correlations between measurements obtained from the same eye, section, and stain. To account for potential nonlinearities in the relationships between crimp parameters and age, we considered three transforms for each parameter: no transform (linear), logarithmic, and square-root. The best-fit transformation was identified using the Akaike information criterion (AIC), a measure of the goodness of fit relative to the complexity of the model. Lower AIC values are preferred. Note that the significance of the model is determined from the LME models, not AIC. For the pooled regions, we used alpha = 0.01 to establish significance.

Regional Comparisons. Pairwise Mann-Whitney-Wilcoxon tests were conducted to test for differences in waviness, tortuosity, and amplitude between each of the eight regions. The original desired significance level was alpha = 0.01. However, because this test was done 28 times, for each pairwise combination of the eight regions, we used a Bonferroni-corrected significance level of alpha = 0.000357 to determine significance. The analyses were repeated using pairwise t-tests and the same results were obtained.

Regional Crimp Parameter Associations With Age. In each of the eight regions, we determined if each of the crimp parameters monotonically increased or decreased with age, as well as if there were significant changes with age. As with the whole globe, we assessed monotonic changes in the crimp parameters with age using Spearman tests and significant age-related changes using LME models. Again, we considered three transforms for each parameter: no transform (linear), logarithmic, and square-root. The best-fit transformation was identified using the AIC value. Because we tested the eight regions individually, we used a Bonferroni-corrected alpha = 0.00125.

Results

We analyzed a minimum of 550 collagen bundles in each of the eight regions. These came from 42 sections taken from the 20 eyes of 20 subjects, spanning 17 specific ages ranging from 0.08 (1 month) to 97 years old. Individual regions were excluded from analysis in the case of tissue tears or folds apparent in the image of the given region. Regardless of number of collagen bundles sampled (20, 30, 40, or 50), the waviness, tortuosity, and amplitude values were similar ($P > 0.1$), as shown by the results from 20 and 50 in Supplementary Figure S1. Equivalent results were observed for other regions and subjects (results not shown). Sections with different stains (see Methods) also yielded similar waviness, tortuosity, and amplitude values, showing that the measurement of the crimp parameters was robust to the stain ($P > 0.1$; Supplementary Fig. S2). Comparable results were obtained for the other subjects and regions (results not shown).

Trends with age were first assessed in the whole globe. We found that the three crimp parameters, waviness, tortuosity, and amplitude, significantly decreased monotonically ($P < 0.01$) with age when pooling the data across all regions of the eye (Fig. 5). For all three transformations of each crimp parameter, we found a significant association with age ($P < 0.01$). For tortuosity and amplitude, the square-root transformation model had the lowest AIC, whereas for waviness, the linear (no transformation) model had the lowest AIC. We repeated the statistical analysis splitting the data into two age groups: 2 years old and older, and younger than 2 years. The parameter decreases with age were significant for both groups. When the data were analyzed separated into eight regions, we found similar results on the crimp parameter associations with age. The waviness, tortuosity, and amplitude in each of the eight regions also significantly decreased monotonically with age ($P < 0.00125$).

We found similar regional trends across the globe for each of the three crimp parameters when considering all subjects pooled (Fig. 6). The equator and limbus showed both the largest values and the largest variabilities for waviness, tortuosity, and amplitude. These trends also held when considering the subjects in two groups: youth (0–17 years) and adults (18–97 years) (Fig. 7). Aside from the values and variabilities decreasing from youth to adults, the largest difference was the change in the limbus with respect to the other regions. Waviness and tortuosity yielded very similar trends in terms of the pairwise comparisons between the eight regions (Fig. 8). We did not find statistically significant differences in any of the three crimp parameters between the posterior sclera and posterior equator, between the limbus and the equator, and between the central cornea and peripheral cornea ($P > 0.1$).

The LME models were used to model and assess the significance of the parameter associations with age. For all three parameters, the posterior equator, anterior equator, and limbus had significant associations with age ($P < 0.00125$; Fig. 9) when modeled with the global linear transform (no transform) for waviness, square-root transform for tortuosity, and square-root transform for amplitude. In the PPS, only amplitude had a significant association with age when modeled with the square-root transform.

When comparing the slopes from the LME models with lowest AIC, or the rate of each region's crimp parameter change with age, we found that the limbus consistently had the steepest slope of all three crimp parameters (Fig. 5). The waviness, tortuosity, and amplitude of the fibers in the limbus region were consistently highest at the youngest ages and decreased fastest with age. For amplitude, the intercepts of the

Investigative Ophthalmology & Visual Science

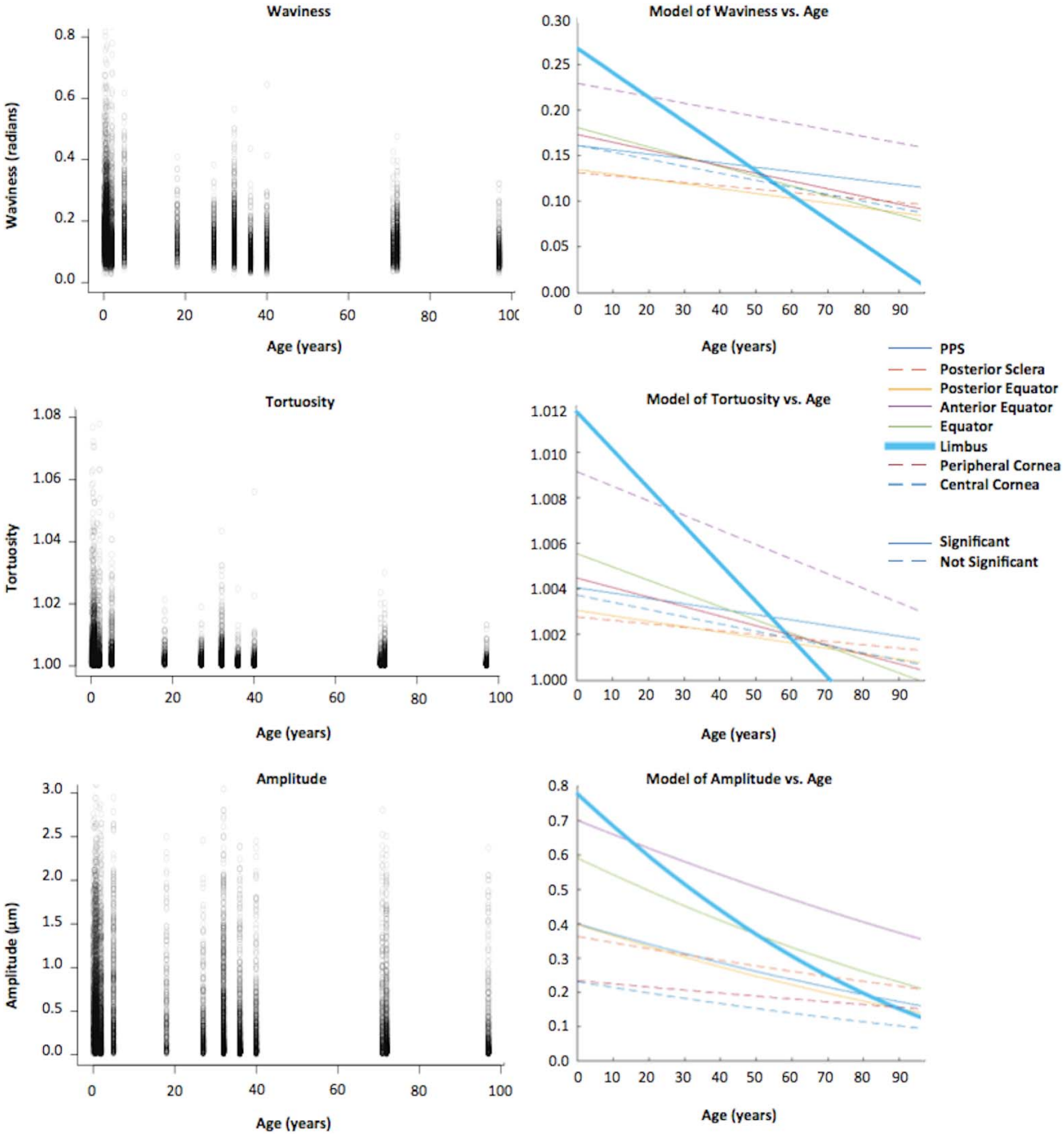

Figure 5. Parameters versus age. The left column shows scatter plots of crimp parameters with age, pooled across all regions in the eye. Ages ranged from 0.08 (1 month) to 97 years, with a slight concentration of samples below 2 years old. At all ages, the variability was larger for amplitude than for waviness and tortuosity. All three parameters had a significant monotonic decrease with age in all regions of the globe pooled ($P < 0.01$). The *right column* shows models of waviness, tortuosity, and amplitude with age. Although all crimp parameters measured decreased with age in every region, the rate of decrease varied from region to region (*colored lines*). Model refers to LME model. The limbus region showed the largest rate decrease with age in all three parameters (*bolded blue line*). For every region, different transformations were tested to determine the best-fit model. We found that of the transforms tested (linear, logarithmic, and square-root of the crimp parameter), the decrease in waviness with age was linear, whereas the decrease in tortuosity and amplitude with age was best described using the square-root transformation of the crimp parameter.

models were much more variable between regions, compared with the intercepts of the waviness and tortuosity. On average, the slope for the limbus was 4.0 times that of the other regions for waviness, 4.5 times for tortuosity, and 2.5 times for amplitude (Fig. 6).

Discussion

The purpose of this study was to measure collagen crimp waviness, tortuosity, and amplitude throughout the human globe and determine how these properties change with

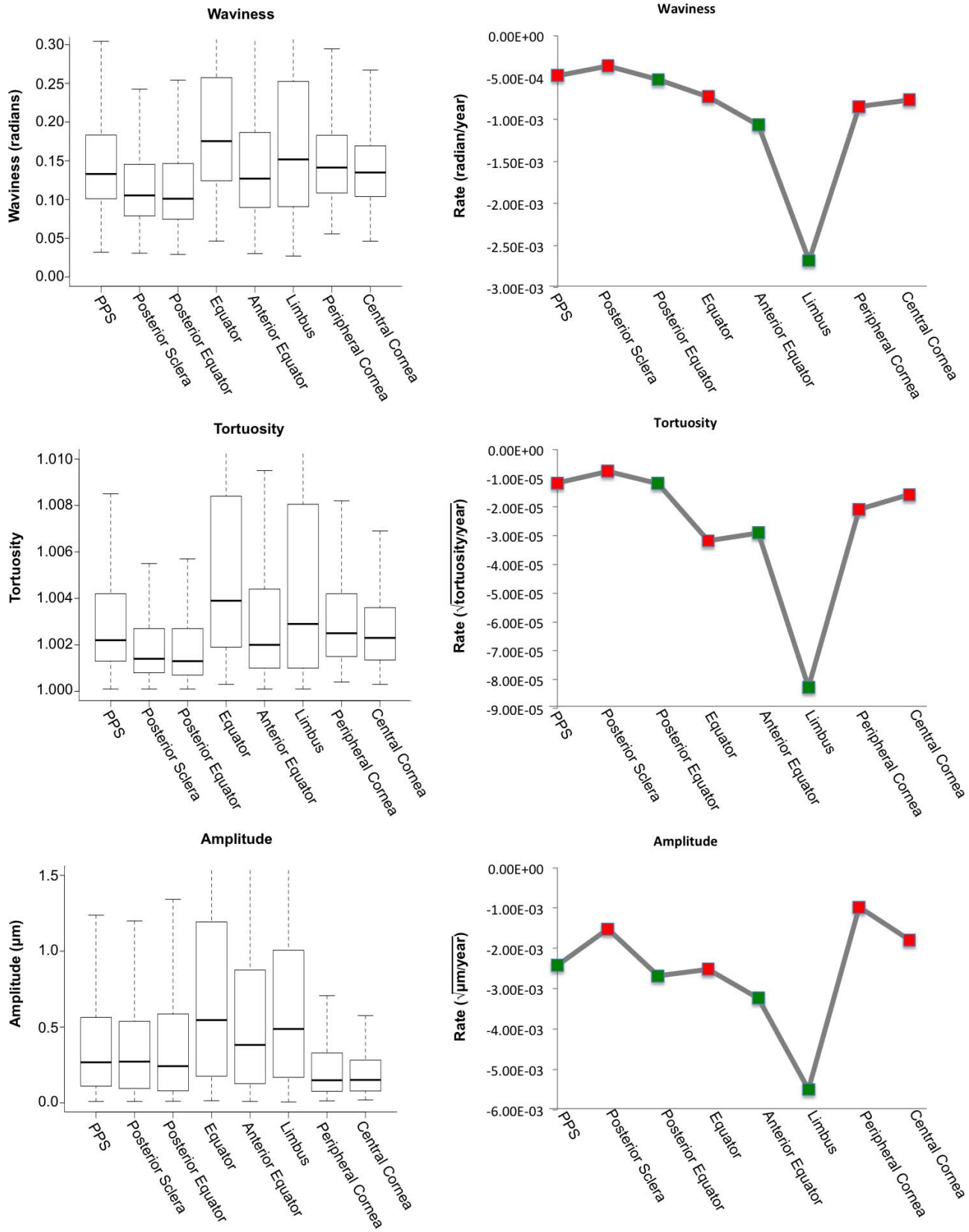

Figure 6. Regional trends. The *left column* shows box plots of waviness, tortuosity, and amplitude grouped by region, from the most posterior region (PPS) to the most anterior region (central cornea) in the eye. The equator and limbus show the largest variability for each parameter. The *right column* shows the relative rates of change and significance for waviness, tortuosity, and amplitude with age in each region. Note that all the rates were negative, indicating that the parameters were always decreasing with age and that the rate of change for the limbus was several times larger than that of any other region for each parameter. *Green points* indicate that the relationship found using the optimal tested transform was determined to be statistically significant ($P < 0.00125$), *red* indicates it was not.

Investigative Ophthalmology & Visual Science

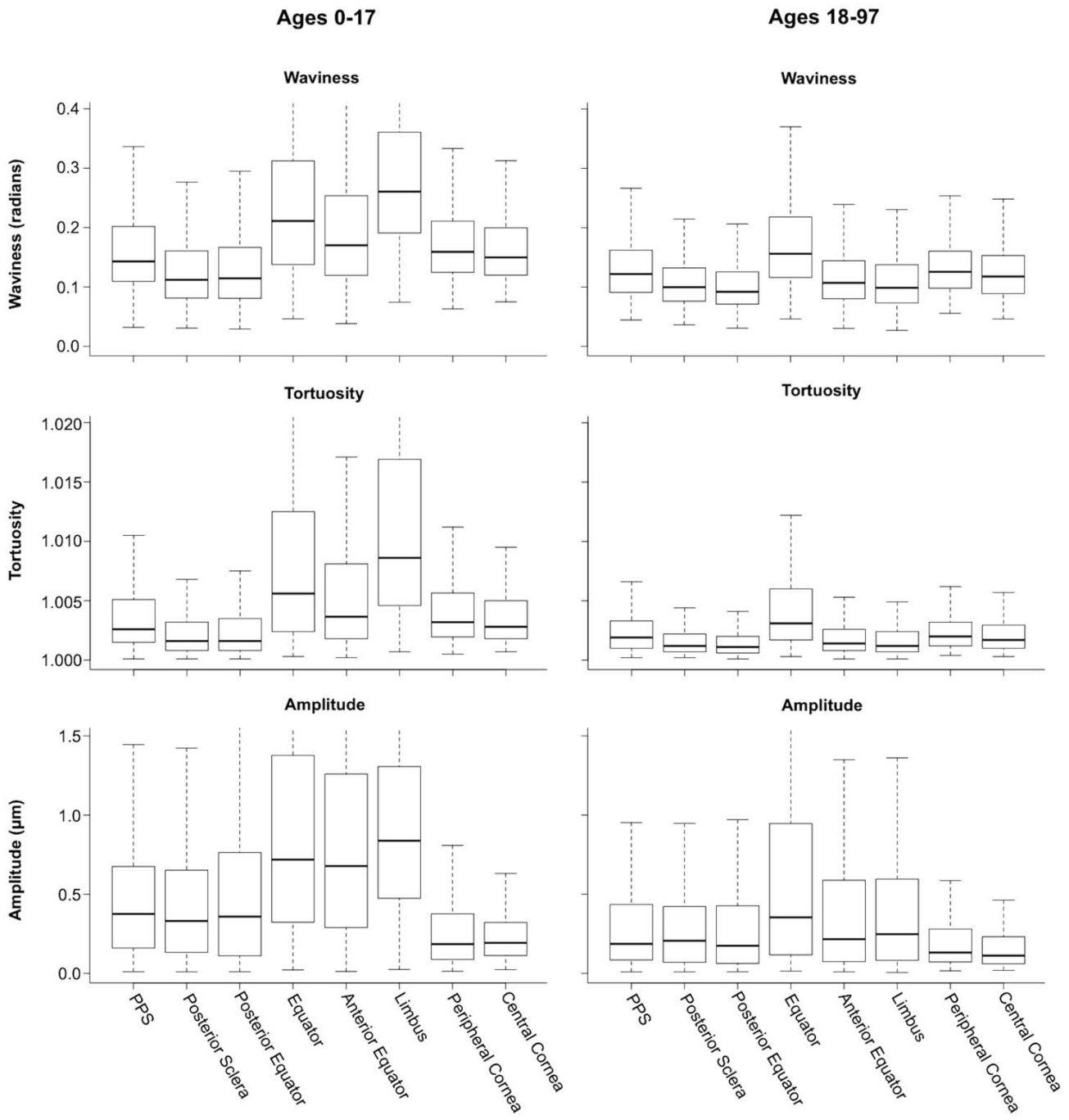

Figure 7. Boxplots of waviness, tortuosity, and amplitude from the posterior to the anterior of the globe. The plots on the *left* are the trends across the globe in youth (ages 0–17) and the plots on the *right* are the trends in adults (18–97). There are similar decreases in both medians and range for all of the regions except the limbus.

age. We characterized the three parameters of collagen crimp in eight regions of the globe of human subjects ranging in ages from 0.08 (1 month) to 97 years. To the best of our knowledge, this is the first systematic experimental quantification of collagen crimp around the globe in humans and the first direct set of measurements of how it changes with age. Three main results arise from this work. First, fiber waviness, tortuosity, and amplitude in the human eye were not uniform. Second, fiber waviness, tortuosity, and amplitude decreased with age, with significantly different age-related decreases between regions. Third, the crimp morphology of the limbus changed the most drastically with age compared with other regions of the eye. Below we discuss each of these in turn.

Investigative Ophthalmology & Visual Science

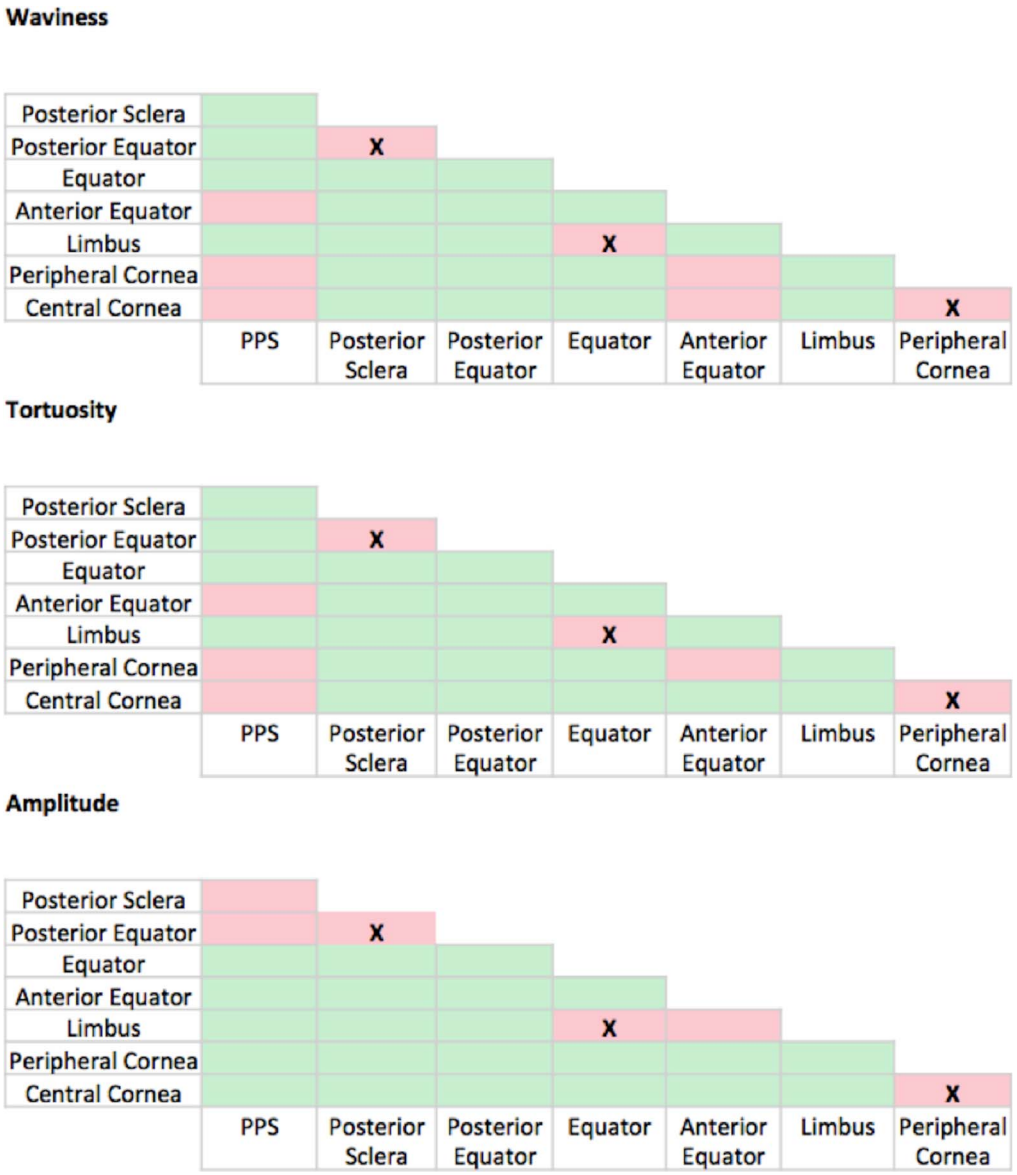

Figure 8. Pairwise Mann-Whitney-Wilcoxon tests comparing the crimp parameters between regions. The tests were used to compare the waviness, tortuosity, and amplitude between each of the eight regions to one another, resulting in 28 tests per parameter. Regions varied substantially. *Green boxes* indicate the presence of significant differences between the regional pair ($P < 0.000357$) and *red boxes* indicate the lack of significant differences ($P > 0.000357$). The X's indicate the three boxes that are *red* in all three panels that were not significantly different.

Fiber Waviness, Tortuosity, and Amplitude Were Not Uniform Over the Human Globe

We found significant differences in at least one crimp parameter for 25 of the 28 region pairings. This underscores the importance of splitting the eye globe into multiple regions for study. It also suggests that the regions are susceptible in different ways to deformations and other stressors affecting crimp. The equator and limbus have both the most crimp and greatest distribution of crimp.

The differences we found between the collagen crimp in the regions of the globe agree with previous studies of regional differences in collagen crimp. In a prior study, we measured collagen crimp around the globe in several 2-year-old sheep[38] by characterizing differences in waviness, tortuosity, amplitude, period, and conformity. Although sheep is a useful animal model,[39] with several similarities to human eyes, it is interesting that the waviness, tortuosity, and amplitude values in humans were somewhat lower than in sheep. Human waviness ranges from 0 to 0.6 radians, tortuosity ranges from 1 to 1.02, and amplitude ranges from 0 to 3 μm. Sheep waviness ranges from 0 to 0.8 radians, tortuosity ranges from 1 to 1.08, and amplitude ranges from 0 to 4 μm. Also, both species show similar trends in tortuosity and larger measures of waviness and amplitude around the globe. In both humans and sheep, there are two separate peaks of elevated values between the PPS and central sclera, forming a double-hump or "M"-shape. In both species, one of those peaks occurs in the limbus. They differ because the second peak occurs in the posterior sclera in sheep, whereas it occurs in the equator in humans.

Investigative Ophthalmology & Visual Science

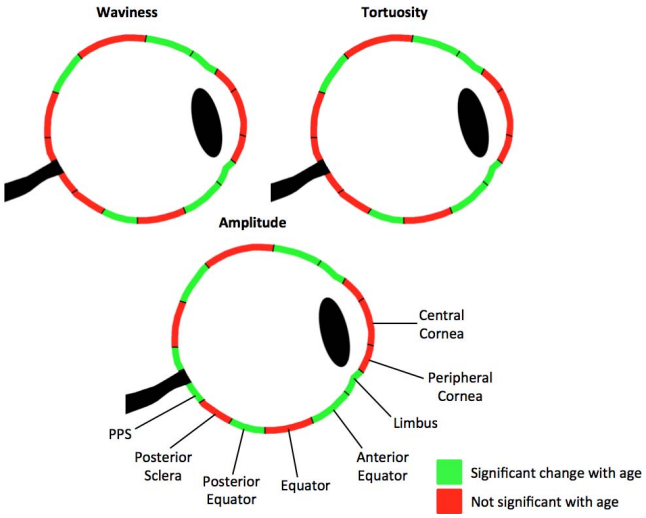

FIGURE 9. Maps of significant associations between waviness, tortuosity, and amplitude with age based on the LME models. *Green* indicates that a significant relationship ($P < 0.00125$) was found between the parameter and age using the global transform. For tortuosity and amplitude, the global transform was square-root. For waviness, the global transform was linear. *Red* indicates that no significance was found ($P > 0.00125$).

Fiber Waviness, Tortuosity, and Amplitude Decreased With Age, With Significantly Different Age-Related Decreases Between Regions

Both when pooling measurements over the whole globe and within each individual region, we found that the waviness, tortuosity, and amplitude all decreased monotonically with age. These results indicate collagen fibers straightening and losing their crimp with age. When pooling the measurements over all regions, the waviness decreased linearly with age, whereas tortuosity and amplitude decreased nonlinearly with age. The latter two crimp parameters were best characterized as having a square-root relationship with age. All three crimp parameters had significant relationships with age in the posterior equator, anterior equator, and limbus. Amplitude also had a significant relationship with age in the PPS. Because waviness, tortuosity, and amplitude decreased monotonically with age in each of the eight regions, lack of significance in these regions suggests that perhaps the relationship of the parameters with age is more complex than can be accounted for by the transformations considered.

The Crimp Morphology of the Limbus Changed the Most Drastically With Age Compared With Other Regions of the Eye

The waviness of the limbus decreased with age on average 4.0 times as faster than other regions, whereas the tortuosity decreased 4.5 times faster, and the amplitude decreased 2.5 times faster. The collagen bundles of the limbus had the largest waviness, tortuosity, and amplitude during infancy and had the smallest waviness and tortuosity, as well as the second smallest amplitude, in old age. It is not known why this was the case. One possibility is that the limbus region must change more than other regions to adapt to the changing conditions during life. Another option is that other regions may be under tighter control, preventing their change with age. For example, large changes in corneal crimp could affect its transparency, and may, therefore, be suppressed. Although the causes and consequences of the large changes in crimp in the limbus remain unclear, our findings demonstrate that the limbus is unique within the eye in how it ages, and therefore that it should be studied in more detail to better determine its role in the global and local biomechanics.

The age-related decrease in collagen crimp and straightening of collagen fibers with age that we found is consistent with findings from studies of other tissues, tendon in particular. Multiple studies have found that crimp angle decreases and crimp length increases with age, whether it was studied in rat tendon,[33] in horse tendon,[34,40] or in mice tendon.[41] A study on craniofacial tendons in zebrafish found that age-related changes in mechanical function were likely due to loss of nonlinearity, which the authors believe could be due to decreases in collagen crimp.[42] This also suggests that the changes in crimp we found could be linked to changes in the eye's mechanical properties.

Age-related increases in cornea stiffness (decreased elasticity) are well established.[19,43] Whereas these likely involve cross-linking affecting the stromal collagen fibrils,[17] our results suggest that the stiffening may also have a component related to the loss of crimp. Grytz and colleagues[18,44] conducted several cross-sectional studies using inflation experiments and inverse-modeling to estimate how collagen changes with age in donor human eyes. Their results consistently show age-related stiffening of the posterior pole sclera, more markedly in donors of African descent than in donors of European descent.[44] Their modeling suggests that the age-related stiffening may be due to decreases in collagen fibril crimp angle,[18] consistent with our findings here.

Coudrillier and colleagues[23,45] have also done multiple studies of posterior pole mechanics and collagen organization with age. The authors found that age was predictive of a stiffer and thinner sclera and that glaucoma eyes had a different mechanical response than normal eyes, perhaps indicating differences in collagen microstructure, such as crimp. Using wide-angle X-ray scattering (WAXS) the authors also found that with age, the overall PPS collagen architecture was less aligned and was less anisotropic (less stiffness directionality). Girard and colleagues[30] found that the posterior sclera of old monkeys is significantly stiffer than that of young monkeys, athough their techniques did not provide insight into the underlying cause of the changes.

In addition to changes in crimp, it is likely that with age there are also changes in tissue composition, such as changes of total collagen or the proportion of various types of collagen, as Albon and colleagues[46] have shown to be the case for the lamina cribrosa. Further work is needed to determine the relative contributions to the age-related stiffening from changes in collagen composition and crimp.

Although decreases in collagen crimp may contribute to an overall globe lengthening with age, the crimp is very small and the effects are minor. A rough calculation based on the tortuosities we report, assuming a spherical globe predicts that the decrease in crimp could account for less than 0.4% of the change in length, or less than 1 μm per year on average. This is orders of magnitude smaller than what has been measured in children[47] and adults.[48] Hence, lengthening of the eye cannot be explained purely from loss of crimp. Changes in globe length, however, could affect crimp. This may be of interest in the study of conditions of the eye, such as myopia, in which it has been reported that increased axial length is often associated with increased sclera stiffness.[49,50] Note that we used the terms "over age," "age-related," or aging in a purely technical sense of being associated with age. Depending on context, it may be useful to distinguish between changes early in life that could be related to development versus changes later in life potentially associated with senescence.

Investigative Ophthalmology & Visual Science

This work focused on three crimp parameters: waviness, tortuosity, and amplitude. Although these properties may be related to one another, our work here and elsewhere[38] shows that each parameter provides a different perspective on crimp, and that they are not redundant. Future work should look into a better understanding of the parameter relationships, perhaps using even higher resolution imaging techniques that can distinguish individual fibers, such as polarization sensitive second harmonic imaging (Li JJ, et al. *IOVS* 2015;56:ARVO E-Abstract 6157).

We are not the first to report on the structure of the collagen in the eye or visualize it. Other techniques, however, do not typically allow simultaneously the wide field of view, sensitivity, and resolution of PLM. For example, measurements from WAXS,[23,51] and small angle light scattering (SALS)[26] are influenced by both large-scale fiber bundle orientation and microstructural crimp.[52]

An important advantage of our PLM-based technique is that calculation of the crimp parameters is possible even when the crimp wave is not directly discernible. Trace-based techniques require clearly discernible fibers. Similarly, angular resolution in gradient-based orientation analyses is tied to the spatial resolution of the images, and depends on clearly identifiable fibers. This is a major limitation in dense tissues with small crimp, such as the sclera and cornea. PLM, in contrast, has excellent angular resolution at the pixel scale, without the need to distinguish fiber edges. Because of this, we were able to mark anywhere in the interior of the bundles and extract the fiber orientations needed to compute waviness, tortuosity, and amplitude.

In addition to the strengths of our method, it is necessary to consider its limitations. We analyzed tissues that had been histologically processed. There could be artifacts as a result of the fixation or sectioning, including tissue distortion or shrinkage. However, because all the globes and regions were treated the same way, comparing them to one another is still appropriate. Future studies could use tissue fixed with 10% formalin, as it has shown to have minimal effects on the size or shape of ocular tissue at large[53] and small scale,[35] or study crimp without sectioning.[20] Further, the globes were fixed without restoring IOP to a physiologic level, hence the measurements of crimp we report should be taken as those without a substantial load. Elsewhere we have shown that laminar and PPS crimp period were not significantly different between eyes fixed at 0, 5, and 10 mm Hg.[9] Effects of IOP during fixation would have affected the entire globe, making comparisons between regions still of interest. Elsewhere we have also shown that increases in IOP above 10 mm Hg do cause important changes in crimp properties, and, further, that these changes can vary from one region of the eye to another.[10] Future studies should use eyes fixed under carefully controlled IOPs.

There could be artifacts due to staining. However, we did not detect any significant differences between the various stains. This evidence is another advantage of our use of PLM, which allows precise measurement of collagen orientation, and waviness, independent of stain, and even without staining.[35] Colors and hues in histological sectioning can be unreliable, which could affect the reliability of crimp measurement techniques based on fiber tracing.

The analyses were done on axial sections through the ONH, and thus we did not study the superior and inferior sectors of the globe. Future studies should consider distinguishing nasal versus temporal sides, which we did not do. The nasal and temporal sclera have distinct differences between length and thickness.[54] Fazio and colleagues[31] describe differences between the nasal and temporal sectors in PPS mechanics. These differences must be better understood. In addition, the sectioning direction may have influenced the collagen crimp characteristics measured since the tissue is three-dimensional (3D), but our measurements are two-dimensional (2D) projections. Although we were careful to measure collagen fibers and bundles in the section plane, it is likely that they had small out-of-plane angles. In this case, our 2D measures of waviness and tortuosity would be underestimated relative to the 3D variations. As mentioned above, because all eyes were studied using the same methodology, comparisons between regions and eyes is useful. Future studies should be done to determine any potential differences with 3D measurements. This could be done, for example, using sections made with different orientations, or using extensions of PLM that allow 3D measurement of fiber orientation.[55] It also should be considered that our measurements do not correspond to specific fibers. Instead, our measurements represent bundles, lamellae (in the cornea), or groups of fibers, not specific fibers, fibrils, or micro-fibrils. Our findings demonstrate that within all regions there are fibers with a wide diversity of properties. Our focus in this study was on overall analysis and trends with age. The relationships between the values we obtain are as important as their actual magnitude. So, even if the individual values we obtain are different from the in vivo, intact tissue, we are confident that the relationships and trends we report are useful to understand the globe.

This was a cross-sectional study. We studied how the crimp parameters changed between subjects of different ages, not how a given subject's collagen crimp changes as they age. Future studies could use in vivo imaging, such as optical coherence tomography or magnetic resonance imaging, to track how a given individual's collagen crimp changes over time in a longitudinal study.

In conclusion, to the best of our knowledge, we have presented the first systematic experimental quantification of collagen crimp around the eye globe in humans with age. We demonstrated that crimp around the globe is not uniform or homogeneous, but also that it is not random. Instead, there are evident patterns in crimp waviness, tortuosity, and amplitude. We also demonstrated that waviness, tortuosity, and amplitude decrease significantly and substantially with age, all over the globe, but most strongly in the limbal region. This region has the more marked crimp in neonates, yet the properties change with age so that its collagen is least crimped in the elderly. The changes in crimp are therefore a mechanism underlying age-related stiffening of the sclera and cornea that is believed to have a strong influence on sensitivity to IOP and susceptibility to some diseases, such as glaucoma. A stiffer globe will suffer higher fluctuations in IOP and higher stresses at all levels of IOP.

Acknowledgments

Supported by National Institutes of Health R01-EY023966, R01-EY025011, T32-EY017271, and P30-EY008098; Eye and Ear Foundation (Pittsburgh, PA, USA); Stimulating Pittsburgh Research in Geroscience (SPRIG) Program; and Research to Prevent Blindness (support to Department of Ophthalmology, University of Pittsburgh Medical Center, Pittsburgh, PA, USA).

Disclosure: **A. Gogola**, None; **N.-J. Jan**, None; **B. Brazile**, None; **P. Lam**, None; **K.L. Lathrop**, None; **K.C. Chan**, None; **I.A. Sigal**, None

References

1. Drexler W, Morgner U, Ghanta RK, Kartner FX, Schuman JS, Fujimoto JG. Ultrahigh-resolution ophthalmic optical coherence tomography. *Nat Med*. 2001;7:502–507.
2. Fratzl P. *Collagen: Structure and Mechanics*. Boston, MA: Springer Science & Business Media; 2008.

3. Standring S. *Gray's Anatomy: The Anatomical Basis of Clinical Practice*. 41st ed. New York: Elsevier Limited; 2016.
4. Andreo RH, Farrell RA. Corneal small-angle light-scattering theory: wavy fibril models. *J Opt Soc Am*. 1982;72:1479–1492.
5. Gallagher B, Maurice D. Striations of light scattering in the corneal stroma. *J Ultrastruct Res*. 1977;61:100–114.
6. Grytz R, Meschke G. Constitutive modeling of crimped collagen fibrils in soft tissues. *J Mech Behav Biomed Mater*. 2009;2:522–533.
7. Newton RH, Brown JY, Meek KM. Polarized light microscopy technique for quantitatively mapping collagen fibril orientation in cornea. *Proc SPIE Int Soc Opt Eng*. 1996;2926:278–284.
8. Holzapfel GA. Biomechanics of soft tissue. In: Lemaitre J, ed. *Handbook of Materials Behavior Models*. Boston, MA: Academic Press; 2001.
9. Jan NJ, Gomez C, Moed S, et al. Microstructural crimp of the lamina cribrosa and peripapillary sclera collagen fibers. *Invest Ophthalmol Vis Sci*. 2017;58:3378–3388.
10. Jan N-J, Sigal IA. Collagen fiber recruitment: a microstructural basis for the nonlinear response of the posterior pole of the eye to increases in intraocular pressure. *Acta Biomater*. 2018; 72:295–305.
11. Fata B, Zhang W, Amini R, Sacks MS. Insights into regional adaptations in the growing pulmonary artery using a meso-scale structural model: effects of ascending aorta impingement. *J Biomech Eng*. 2014;136:021009–021013.
12. Hansen KA, Weiss JA, Barton JK. Recruitment of tendon crimp with applied tensile strain. *J Biomech Eng*. 2001;124:72–77.
13. Hill MR, Duan X, Gibson GA, Watkins S, Robertson AM. A theoretical and non-destructive experimental approach for direct inclusion of measured collagen orientation and recruitment into mechanical models of the artery wall. *J Biomech*. 2012;45:762–771.
14. Ethier CR, Johnson M, Ruberti J. Ocular biomechanics and biotransport. *Annu Rev Biomed Eng*. 2004;6:249–273.
15. Grytz R, Meschke G, Jonas JB. The collagen fibril architecture in the lamina cribrosa and peripapillary sclera predicted by a computational remodeling approach. *Biomech Model Mechanobiol*. 2011;10:371–382.
16. Burgoyne CF. A biomechanical paradigm for axonal insult within the optic nerve head in aging and glaucoma. *Exp Eye Res*. 2011;93:120–132.
17. Elsheikh A, Wang D, Brown M, Rama P, Campanelli M, Pye D. Assessment of corneal biomechanical properties and their variation with age. *Curr Eye Res*. 2007;32:11–19.
18. Grytz R, Fazio MA, Libertiaux V, et al. Age- and race-related difference in human scleral material properties. *Invest Ophthalmol Vis Sci*. 2014;55:8163–8172.
19. Liu B, McNally S, Kilpatrick JI, Jarvis SP, O'Brien CJ. Aging and ocular tissue stiffness in glaucoma. *Surv Ophthalmol*. 2018; 63:56–74
20. Ho LC, Sigal IA, Jan N-J, et al. Magic angle-enhanced MRI of fibrous microstructures in sclera and cornea with and without intraocular pressure loading. *Invest Ophthalmol Vis Sci*. 2014;2:522–533.
21. Jan N-J, Lathrop K, Sigal IA. Collagen architecture of the posterior pole: high-resolution wide field of view visualization and analysis using polarized light microscopy. *Invest Ophthalmol Vis Sci*. 2017;58:735–744.
22. Zyablitskaya M, Takaoka A, Munteanu EL, Nagasaki T, Trokel SL, Paik DC. Evaluation of therapeutic tissue crosslinking (TXL) for myopia using second harmonic generation signal microscopy in rabbit sclera. *Invest Ophthalmol Vis Sci*. 2017; 58:21–29.
23. Coudrillier B, Pijanka J, Jefferys J, et al. Collagen structure and mechanical properties of the human sclera: analysis for the effects of age. *J Biomech Eng*. 2015;137:041006.
24. Dupps WJ, Netto MV, Herekar S, Krueger RR. Surface wave elastometry of the cornea in porcine and human donor eyes. *J Refract. Surg*. 2007;23:66–75.
25. Elsheikh A, Geraghty B, Alhasso D, Knappett J, Campanelli M, Rama P. Regional variation in the biomechanical properties of the human sclera. *Exp Eye Res*. 2010;90:624–633.
26. Girard MJ, Dahlmann-Noor A, Rayapureddi S, et al. Quantitative mapping of scleral fiber orientation in normal rat eyes. *Invest Ophthalmol Vis Sci*. 2011;52:9684–9693.
27. Clayson K, Pan X, Pavlatos E, et al. Corneoscleral stiffening increases IOP spike magnitudes during rapid microvolumetric change in the eye. *Exp Eye Res*. 2017;165:29–34.
28. Stowell C, Burgoyne C, Tamm ER, Ethier CR; Lasker/IRRF Initiative on Astrocytes and Glaucomatous Neurodegeneration Participants. Biomechanical aspects of axonal damage in glaucoma: a brief review. *Exp Eye Res*. 2017;157:13–19.
29. Voorhees AP, Ho LC, Jan N-J, et al. Whole-globe biomechanics using high-field MRI. *Exp Eye Res*. 2017;160:85–95.
30. Girard MJA, Suh JKF, Bottlang M, Burgoyne CF, Downs JC. Scleral biomechanics in the aging monkey eye. *Invest Ophthalmol Vis. Sci*. 2009;50:5226–5237.
31. Fazio MA, Grytz R, Morris JS, et al. Age-related changes in human peripapillary scleral strain. *Biomech Model Mechanobiol*. 2014;13:551–563.
32. Tuite D, Renstrom P, O'Brien M. The aging tendon. *Scand J Med Sci Sports*. 1997;7:72–77.
33. Diamant J, Keller A, Baer E, Litt M, Arridge RGC. Collagen; ultrastructure and its relation to machanical properties as a function of ageing. *Proc R Soc Lond B Biol Sci*. 1972;180:293–315.
34. Patterson-Kane J, Firth E, Goodship A, Parry D. Age-related differences in collagen crimp patterns in the superficial digital flexor tendon core region of untrained horses. *Aust Vet J*. 1997;75:39–44.
35. Jan N-J, Grimm JL, Tran H, et al. Polarization microscopy for characterizing fiber orientation of ocular tissues. *Biomed Opt Express*. 2015;6:4705–4718.
36. Schindelin J, Arganda-Carreras I, Frise E, et al. Fiji: an open-source platform for biological-image analysis. *Nat Methods*. 2012;9:676–682.
37. Yang B, Jan N-J, Brazile B, Voorhees A, Lathrop KL, Sigal IA. Polarized light microscopy for 3-dimensional mapping of collagen fiber architecture in ocular tissues [published online ahead of print April 6, 2018]. *J Biophotonics*. doi:10.1002/jbio.201700356.
38. Jan N-J, Brazile BL, Hu D, et al. Crimp around the globe; patterns of collagen crimp across the corneoscleral shell. *Exp Eye Res*. 2018;172:159–170.
39. Gerometta R, Spiga M-G, Borras T, Candia OA. Treatment of sheep steroid-induced ocular hypertension with a glucocorticoid-inducible MMP1 gene therapy virus. *Invest Ophthalmol Vis Sci*. 2010;51:3042–3048.
40. Patterson-Kane JC, Parry DAD, Birch HL, Goodship AE, Firth EC. An age-related study of morphology and cross-link composition of collagen fibrils in the digital flexor tendons of young thoroughbred horses. *Connect Tissue Res*. 1997;36: 253–260.
41. Legerlotz K, Dorn J, Richter J, Rausch M, Leupin O. Age-dependent regulation of tendon crimp structure, cell length and gap width with strain. *Acta Biomater*. 2014;10:4447–4455.

Investigative Ophthalmology & Visual Science

42. Shah RR, Nerurkar NL, Wang C, Galloway JL. Tensile properties of craniofacial tendons in the mature and aged zebrafish. *J Orthop Res*. 2015;33:867–873.
43. Studer H, Larrea X, Riedwyl H, Buchler P. Biomechanical model of human cornea based on stromal microstructure. *J Biomech*. 2010;43:836–842.
44. Fazio MA, Grytz R, Morris JS, Bruno L, Girkin CA, Downs JC. Human scleral structural stiffness increases more rapidly with age in donors of African descent compared to donors of European descent. *Invest Ophthalmol Vis Sci*. 2014;55:7189–7198.
45. Coudrillier B, Tian J, Alexander S, Myers KM, Quigley HA, Nguyen TD. Biomechanics of the human posterior sclera: age- and glaucoma-related changes measured using inflation testing. *Invest Ophthalmol Vis Sci*. 2012;53:1714–1728.
46. Albon J, Karwatowski WS, Avery N, Easty DL, Duance VC. Changes in the collagenous matrix of the aging human lamina cribrosa. *Br J Ophthalmol*. 1995;79:368–375.
47. Capozzi P, Morini C, Piga S, Cuttini M, Vadala P. Corneal curvature and axial length values in children with congenital/infantile cataract in the first 42 months of life. *Invest Ophthalmol Vis Sci*. 2008;49:4774–4778.
48. Atchison DA, Markwell EL, Kasthurirangan S, Pope JM, Smith G, Swann PG. Age-related changes in optical and biometric characteristics of emmetropic eyes. *J Vis*. 2008;8(4):29.
49. Grytz R, El Hamdaoui M. Multi-scale modeling of vision-guided remodeling and age-dependent growth of the tree shrew sclera during eye development and lens-induced myopia. *J Elast*. 2017;129:171–195.
50. Metlapally R, Wildsoet CF. Scleral mechanisms underlying ocular growth and myopia. *Prog Mol Biol Transl Sci*. 2015;134:241–248.
51. Pijanka JK, Coudrillier B, Ziegler K, et al. Quantitative mapping of collagen fiber orientation in non-glaucoma and glaucoma posterior human sclerae. *Invest Ophthalmol Vis Sci*. 2012;53:5258–5270.
52. Pierlot CM, Lee JM, Amini R, Sacks MS, Wells SM. Pregnancy-induced remodeling of collagen architecture and content in the mitral valve. *Ann Biomed Eng*. 2014;42:2058–2071.
53. Tran H, Jan N-J, Hu D, et al. Formalin fixation and cryosectioning cause only minimal changes in shape or size of ocular tissues. *Sci Rep*. 2017;7:12065.
54. Norman RE, Flanagan JG, Rausch SMK, et al. Dimensions of the human sclera: thickness measurement and regional changes with axial length. *Exp Eye Res*. 2010;90:277–284.
55. Yang B, Jan N, Brazile B, Voorhees A, Lathrop KL, Sigal IA. Polarized light microscopy for 3D mapping of collagen fiber architecture in ocular tissues. *J Biophotonics*. 2018:e201700356.

Investigative Ophthalmology & Visual Science